Supporting Information

Homogenizing Li^+ transport in high-loading sulfur cathodes enabled by synergy of all-in-one thin electrode design and a multifunctional binder for practical Li-S batteries

Hongjiang Song,[a] Shengkui Zhong,[b] Jie Liu*[a] and Shanqing Zhang*[c]

[a] Youth Innovation Team of Shandong Higher Education Institutions, College of Chemical Engineering, Qingdao University of Science and Technology, Qingdao 266042, Shandong, China

[b] School of Green Building and Low-Carbon Technology, Guangxi Technological College of Machinery and Electricity, Nanning 530007, Guangxi, China

[c] School of Chemical Engineering and Light Industry, Guangdong University of Technology, Guangzhou 510006, China

* Corresponding authors. E-mail: jie.liu@qust.edu.cn (Jie Liu); s.zhang@gdut.edu.cn (Shanqing Zhang)

Experimental section

Materials

All chemicals were used without additional purification. 1.0 M LiTFSI in DOL/DME mixture (1:1 Vol%) with 2.0% $LiNO_3$ was purchased from Duoduo Chemical Technology Co., Ltd. Super P was purchased from Temigao Graphite Co., Ltd. Flaxseed gum (FG) was purchased from Xinjiang Linseed Biologic Technology Co., Ltd. 4-hydroxy-6-methyl-3-nitro-2-pyridone (NP, ≥ 97%) and sulfur powders were purchased from Aladdin. Polyvinylidene difluoride (PVDF) was purchased from Canrd Technology Co., Ltd. Li foils (≥ 99.99%) were purchased from Xinghua Benote Battery Materials Co., Ltd. Celgard 2500 separator was purchased from Sinero Technology Co., Ltd.

Characterizations

The functional groups of samples were examined using Fourier transform infrared spectroscopy (FTIR, Nicolet iS10). X-ray photoelectron spectroscopy (XPS) was carried out on Thermo Scientific Escalab 250 Xi spectrophotometer with Al Kα radiation as the X-ray source, and was referenced to the C 1s peak (284.8 eV). Scanning electron microscopy (SEM, JSM-6700F) was used to characterize the surface morphology. Adhesion, energy dissipation, and Young's modulus were precisely measured using atomic force microscopy (AFM, Bruker Dimension Icon). The contact angles of the S@FG-NP AE and S@PVDF CE toward Li-S battery electrolyte were tested using a contact angle meter (JY-82C). In situ Raman spectra were recorded on Renishaw InVia Qontor spectrophotometer with a laser of 532 nm.

All UV-vis spectra were recorded on a UV-vis spectrophotometer (Metash, UV-8000).

Adsorption capability test

Polysulfide adsorption: The Li_2S_6 solution was prepared by mixing sulfur and lithium sulfide (Li_2S) at a molar ratio of 5:1 into a DOL/DME mixture (1:1 Vol%) and stirring overnight at 70 °C in an Ar-filled glovebox. Next, FG, NP, and FG-NP were mixed with Super P in an aqueous solution at a weight ratio of 6:4, followed by drying. Then, 160 mg of FG/Super P, NP/Super P, and FG-NP/Super P powders were added into three glass bottles with 2 mM Li_2S_6 solutions, respectively. After standing for 48h, the supernatant liquid was injected into a quartz cuvette and sealed in the glove box. Then the supernatant was analyzed using a UV-vis spectrophotometer. Li_2S_6 adsorption test for PVDF/Super P powder was carried out as the reference under the same conditions, except using NMP as solvent.

Catalytic capability evaluation

Li_2S nucleation and dissolution experiments: The Li_2S_8 catholyte was prepared by mixing sulfur and Li_2S at a molar ratio of 7:1 into a DOL/DME mixture (1:1 Vol%) and stirring overnight at 65 °C in an Ar-filled glovebox. The working electrodes were prepared by mixing Super P and polymers by a weight ratio of 6:4. Then, 20 μL Li_2S_8 catholyte (0.5 M) and 20 μL blank electrolyte were added into the working electrode side and the Li anode side, respectively. The cells were discharged to 2.06 V at 0.1 C and then discharged at 2.04 V until the current is lower than 0.03 mA for Li_2S nucleation and growth. For Li_2S dissolution, the cells were first discharged galvanostatically at 0.112 mA to 1.8 V, and then charged potentiostatically at 2.4 V.

Symmetrical cells: The electrode was prepared by mixing Super P and polymers by a weight ratio of 6:4. The symmetrical cells were assembled using the above electrode as both anode and cathode with 40 μL Li_2S_6 catholyte (0.1 M). Then CV curves of symmetrical cells were recorded at a scan rate of 10 mV s^{-1} (voltage range from −1.0 V to 1.0 V).

Relative active energy calculation: The relative activation energies of S@FG-NP AE and S@PVDF CE could be calculated according to equation S1:

$$E_{a,Red} = E_{a,Red}^{0} + \alpha zF\varphi_{cathode}(Ox/Red)_{IR} \quad \text{(S1)}$$

where $E_{a,Red}$ refers to the activation energy of the reduction procedure, $E_{a,Red}^{0}$ refers to the intrinsic activation energy, α is the symmetry coefficient, Z is the number of electron transfer, F is the Faraday's constant, and φ is the irreversible potential in the reduction process.

The Tafel curve is described by:

$$\eta_{cathode} = \frac{RT}{\alpha zF} lnj_0 - \frac{RT}{\alpha zF} lnj_{cathode} \quad \text{(S2)}$$

Where $\eta_{cathode}$ is the overpotential of cathode, R is the molar gas constants, j_0 is the exchange current density, $j_{cathode}$ is the current of cathode. The formula can be further simplified as：

$$\eta_{cathode} = a + b\, lnj_{cathode} \quad \text{(S3)}$$

$$a = \frac{RT}{\alpha zF} lnj_0 \quad \text{(S4)}$$

$$b = -\frac{RT}{\alpha zF} \quad \text{(S5)}$$

where a refers to the intercept of the Tafel curve, b is the slope of the Tafel curve.

Based on the formula S3, S4, and S5, the equation S1 can be written as S6：

$$E_{a,Red} = E_{a,Red}^{0} - \frac{RT}{b}\varphi_{cathode}(Ox/Red)_{IR} \quad \text{(S6)}$$

Electrode fabrication

All-in-one electrode (AE): For the preparation of AE with different sulfur content, the FG and NP mixture (2:8), sulfur powder, and Super P were mixed in a mass ratio of 15:50:35, 15:65:20. For the lean-binder AE, the FG and NP mixture, sulfur powder, and Super P were mixed in a mass ratio of 2.5:62.5:35. Subsequently, the mixture was stirred in deionized water to further mix uniformly, and then dried at 60 °C for 5 h. The dried composite was heated at 155 °C for 12 h under Ar condition to obtain the dense cathode material (S@FG-NP). The S@FG-NP powders were dispersed in deionized water and coated onto carbon-coated Al foil/carbon paper. After drying in a vacuum oven at 60 °C for 12h, the S@FG-NP AE was achieved.

Conventional electrode (CE): For the preparation of the S@FG-NP CE, the sulfur powder and Super P were first mixed with a mass ratio of 62.5:37.5, and then heated at 155 °C for 12 h to obtain the S/C composite material. Then, FG-NP binder was prepared by heating the mixture of FG and NP (2:8) at 155 ℃ for 4h under vacuum. Subsequently, FG-NP binder, the S/C composite, and Super P were mixed in the deionized water in a mass ratio of 15:80:5 to obtain a homogeneous slurry with a sulfur content of 50 wt%. Then the slurry was coated on carbon-coated Al foil/carbon paper and dried at 60 °C for 12h in a vacuum oven. S@FG CE, S@NP CE, and S@PVDF CE were prepared as references.

For the Li-S pouch cell, the cathode sizes were 3.0 × 4.0 cm^2 and 7.0 × 8.0 cm^2.

A double-sided cathode was used to achieve Ah-level pouch cell. The double-sided cathode is fabricated through sequential coating: the lean-binder cathode slurry was first coated onto one side of the carbon paper, after drying, repeated the process on the opposite side. The application of a dual-sided cathode reduces the number of current collectors, which can significantly enhance the total energy density of the battery system.

Electrochemical measurements

The LAND-CT3002A battery measurement system was used for the charge/discharge test of the Li-S batteries in the voltage range of 1.8−2.6 V. Cyclic voltammetry (CV) and electrochemical impedance spectroscopy (EIS) were conducted on an electrochemical workstation (Corrtest CS2350M). The galvanostatic intermittent titration technique (GITT) measurements were carried out by applying a pulse constant current of 0.1 C with a duration of 10 min, followed by 1h relaxation to reach an equilibrium voltage.

Theoretical calculations

All of the calculations based on density functional theory (DFT) were performed by utilizing the DMol3 package. The generalized gradient approximation (GGA) in the Perdew-Burke-Ernzerhof form and the Semicore Pseudopotential method with the double numerical basis setting plus the polarization functional were adopted. A DFT-D correction with the Grimme scheme was used to account for the dispersion interaction. The SCF convergence for each electronic energy was set as 1.0×10^{-6} Ha, and the geometry optimization convergence criteria were set up as follows: 1.0×10^{-5}

Ha for energy, 0.001 Ha $Å^{-1}$ for force, and 0.001 Å for displacement, respectively. The binding energies (E_b) of Li_2S_n (LiPS, n=4, 6, 8) and different binders were calculated based on the following equation:

$$E_b = E_{LiPS} + E_{binder} - E_{LiPS+binder} \quad \text{(S7)}$$

The E_{LiPS}, E_{binder}, $and\ E_{LiPS+binder}$ represent the energy of LiPS, the binder, and the binder adsorbing LiPS, respectively. Crystal Orbital Hamilton Population (COHP) was calculated to quantify the strength of chemical bonds in Li_2S_6. A negative COHP value indicates bonding interactions (stabilizing), while a positive value indicates antibonding interactions (destabilizing). The Gibbs free energy for the sulfur reduction process is calculated as the following formula:

$$\Delta G = \Delta E_{tot} + \Delta ZPE + P\Delta V \quad \text{(S8)}$$

where ΔE_{tot}, ΔZPE, and ΔV are the change in DFT total energy, zero-point energy, and volume from the initial state to the final state, respectively.

Finite element simulation of Li^+ concentration distribution in an electrode used the COMSOL multiphysics software with a lithium-ion battery module. The transport process was described by the time-dependent Nernst–Planck equation, and snapshots of the concentration distribution for the models were captured after a fixed period of electrochemical reaction during the simulation. The initial Li^+ concentration was 1 M. The voltage was set at 2.36 V. The thicknesses of the S@FG-NP AE and the S@PVDF CE were set as 62 μm and 122 μm, respectively.

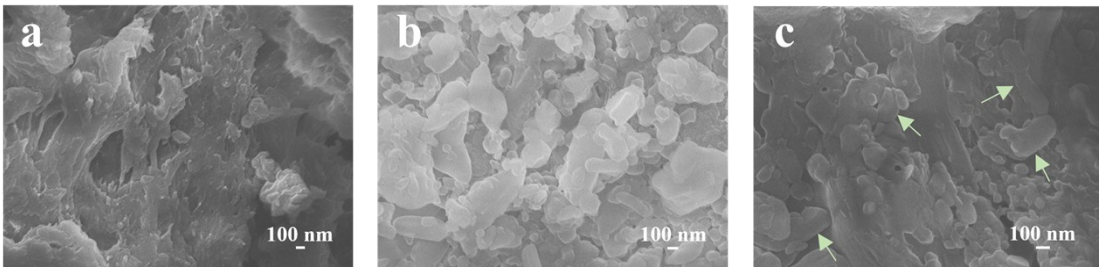

Figure S1 SEM images of (a) FG, (b) NP, and (c) FG-NP (Green arrow represents NP).

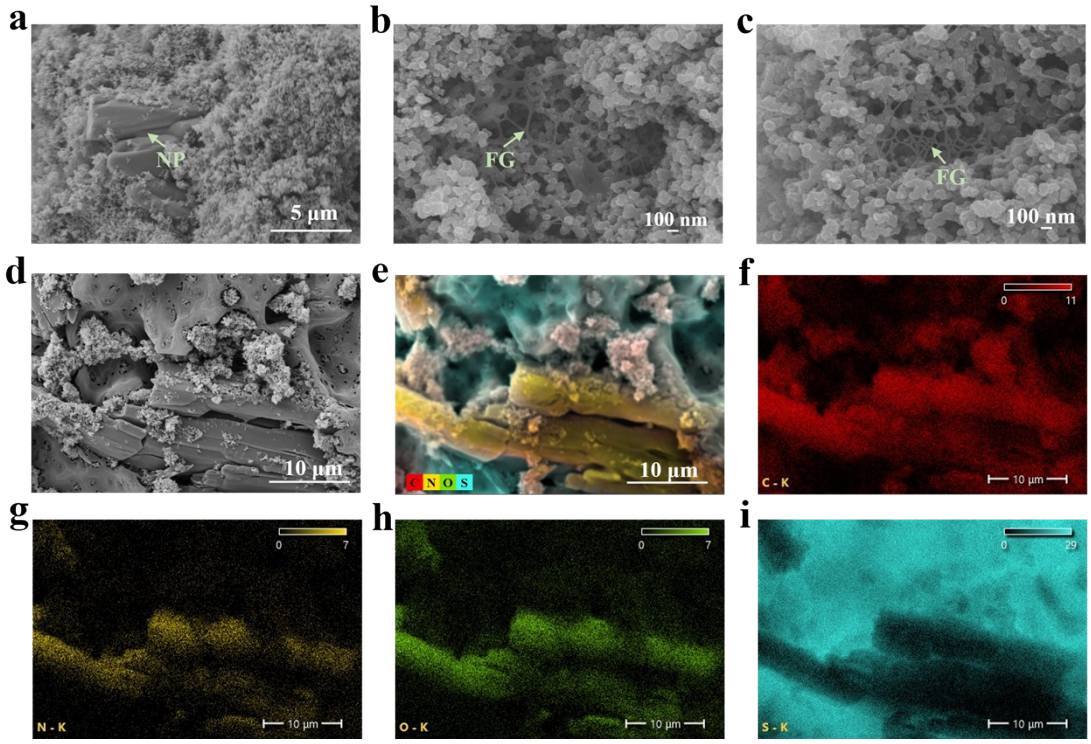

Figure S2 (a-d) SEM images of S@FG-NP AE materials, and (e-i) the corresponding element distribution.

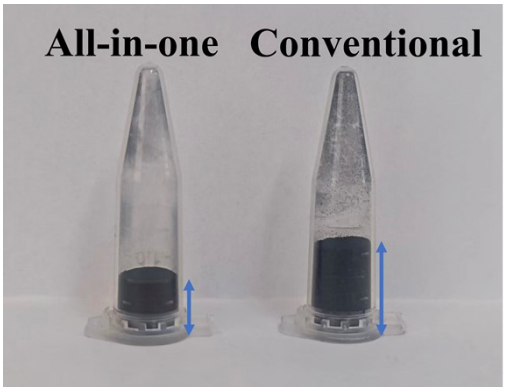

Figure S3 Photograph of S@FG-NP AE materials and S@FG-NP CE materials with the same mass.

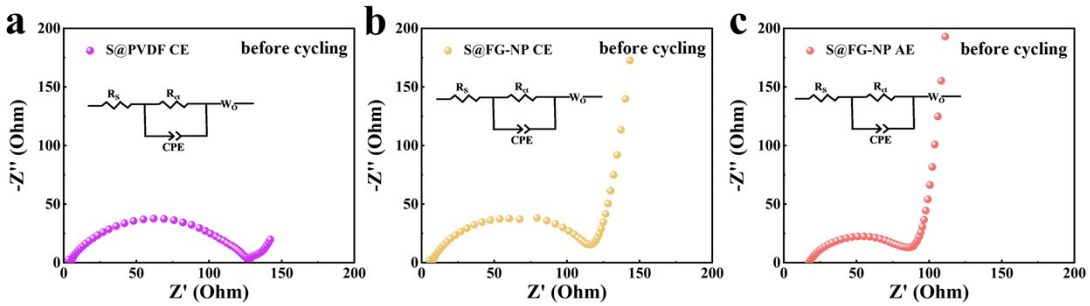

Figure S4 Electrochemical impedance spectra (EIS) of S@PVDF CE, S@FG-NP CE, and S@FG-NP AE before cycling.

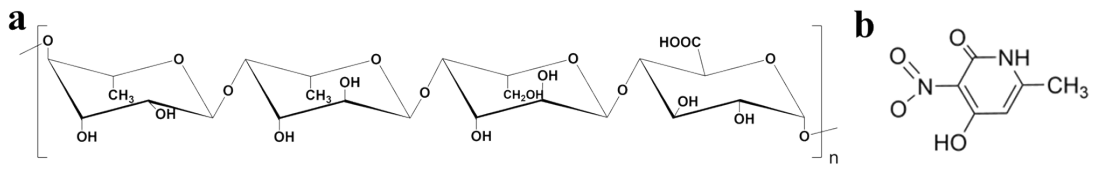

Figure S5 Chemical structure of (a) flaxseed gum (FG) and (b) 4-hydroxy-6-methyl-3-nitro-2-pyridone (NP).

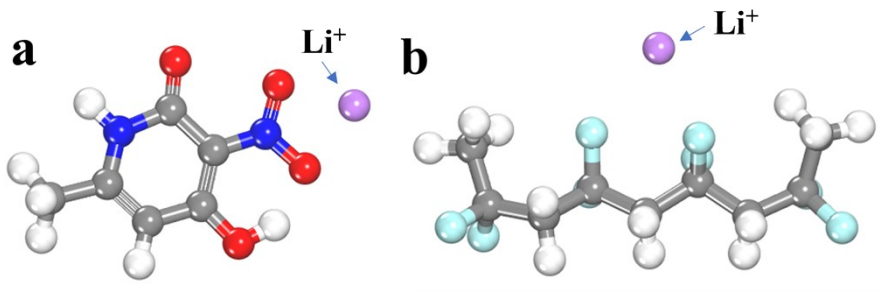

Adsorption Energy= -3.09 eV **Adsorption Energy= -0.19 eV**

Figure S6 Adsorption energy toward Li^+ of (a) NP and (b) PVDF.

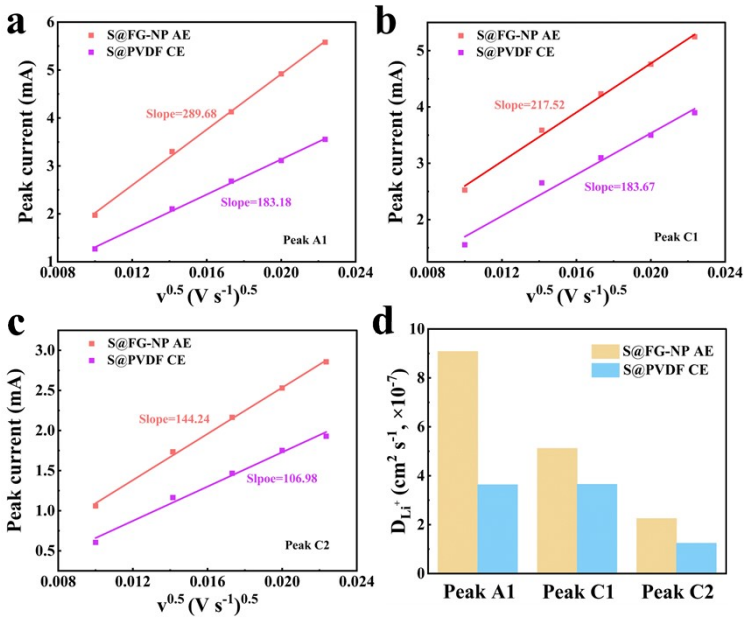

Figure S7 Linear relationship between peak current and the square root of scan rate of S@FG-NP AE and S@PVDF CE for (a) Peak A1, (b) Peak C1, and (c) Peak C2. (d) Apparent Li^+ diffusion coefficients for S@FG-NP AE and S@PVDF CE. The ion diffusion coefficient can be evaluated according to the following equation:

$$D = \left(\frac{I_P v^{-0.5}}{26900 n^{1.5} AC}\right)^2$$

Where I_p represents the peak current, v represents the scan rate, n represents the number of electron transfer, A represents the area of the positive electrode, and C represents the concentration of Li^+.

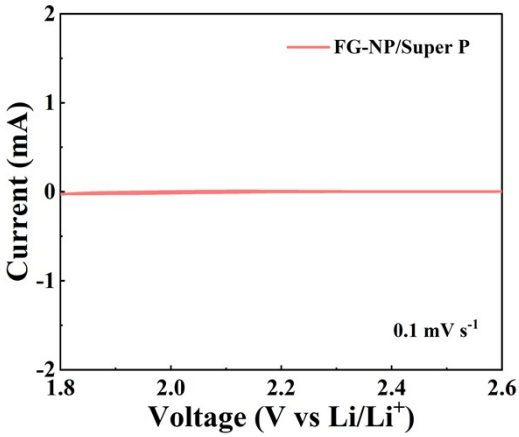

Figure S8 CV curve for the FG-NP/Super P composite electrode at a sweep rate of 0.1 mV s^{-1}.

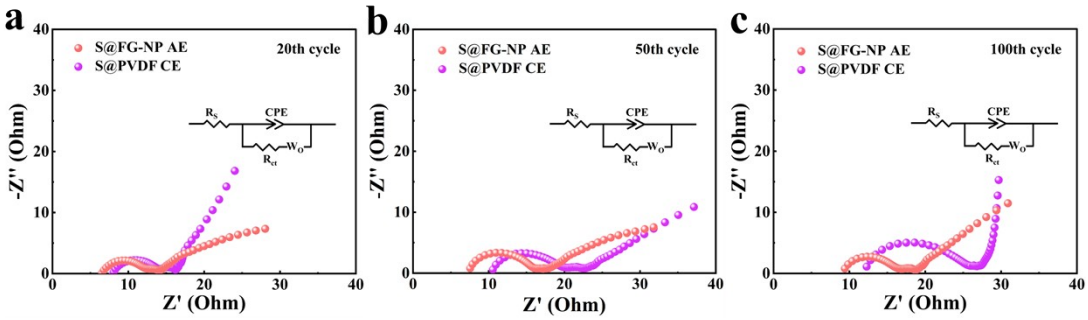

Figure S9 Electrochemical impedance spectra (EIS) of S@FG-NP AE and S@PVDF CE after (a) 20 cycles, (b) 50 cycles, and (c) 100 cycles.

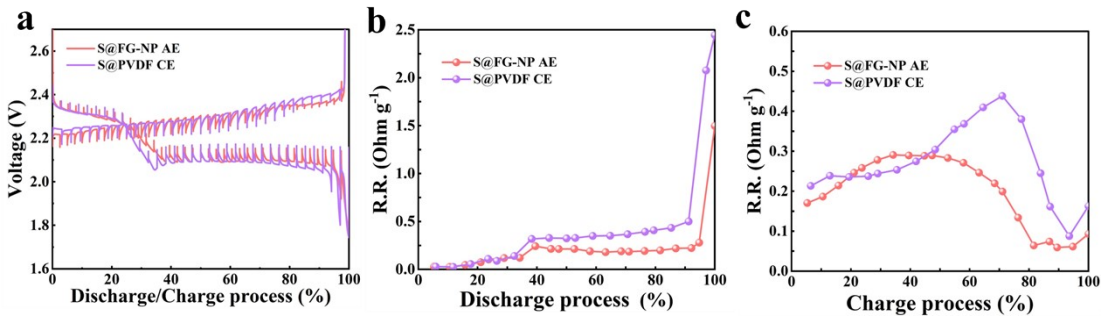

Figure S10 (a) Galvanostatic intermittent titration technique (GITT) curves of S@FG-NP AE and S@PVDF CE at 0.1 C. The corresponding reaction resistance (R.R.) during (b) discharge process and (c) charge process.

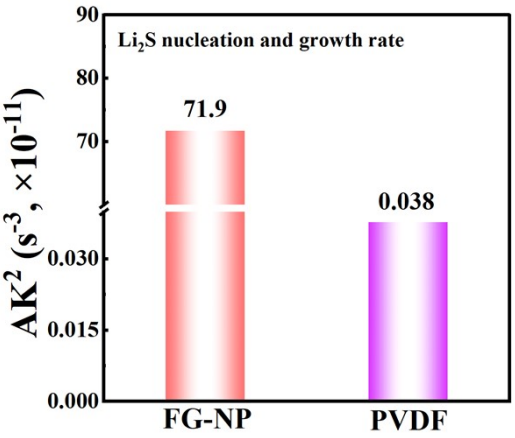

Figure S11 Li_2S nucleation and growth rate on FG-NP and PVDF substrates.

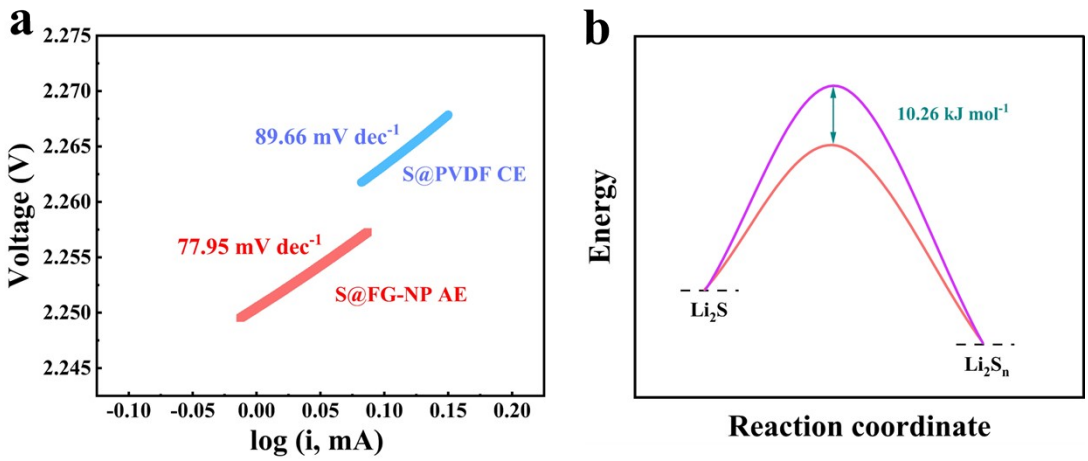

Figure S12 (a) Tafel slopes and (b) calculated activation energy of the Li_2S oxidation process for S@FG-NP AE and S@PVDF CE.

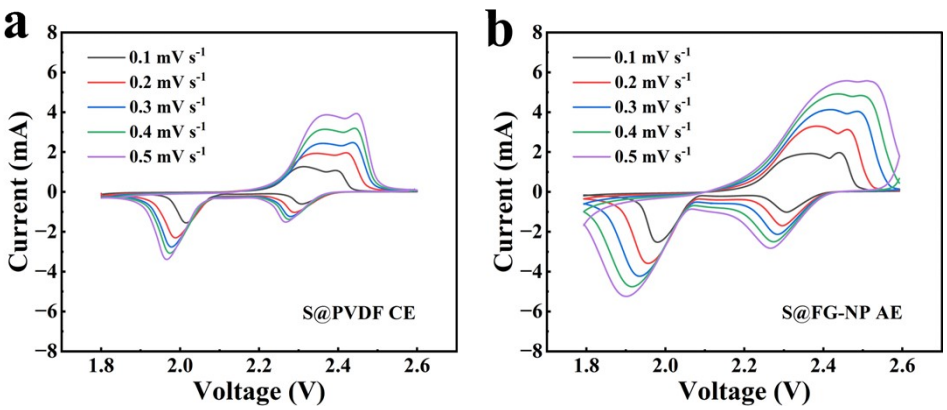

Figure S13 CV curves of (a) S@PVDF CE and (b) S@FG-NP AE at the scan rates of 0.1-0.5 mV s^{-1}.

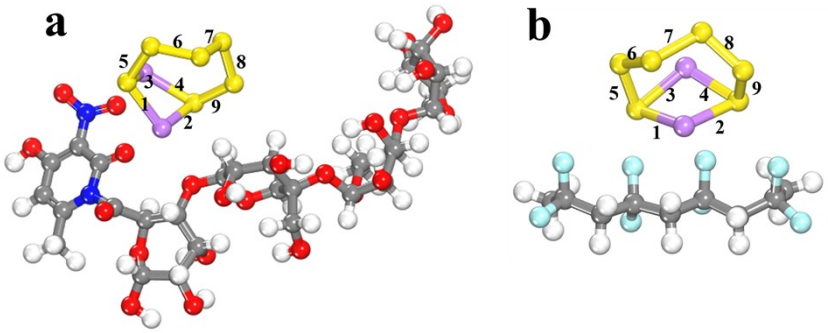

Figure S14 The bond length of the S–S bond and Li-S bond in Li_2S_6 after adsorption on (a) FG-NP binder and (b) PVDF binder.

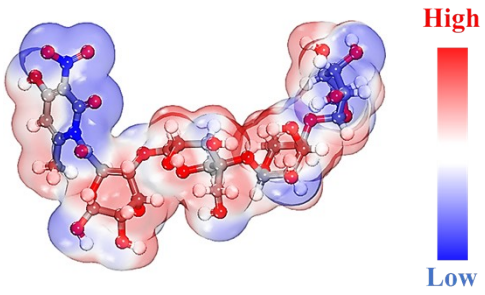

Figure S15 The electrostatic potential distribution of FG-NP.

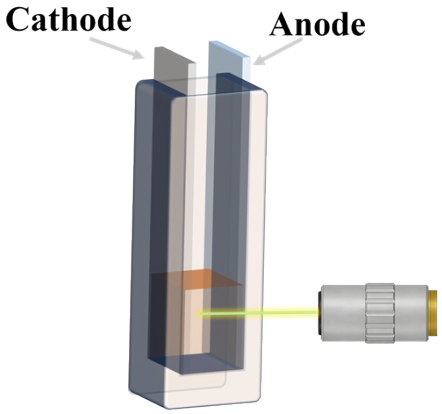

Figure S16 Schematic diagram of the in-situ UV-vis spectra test.

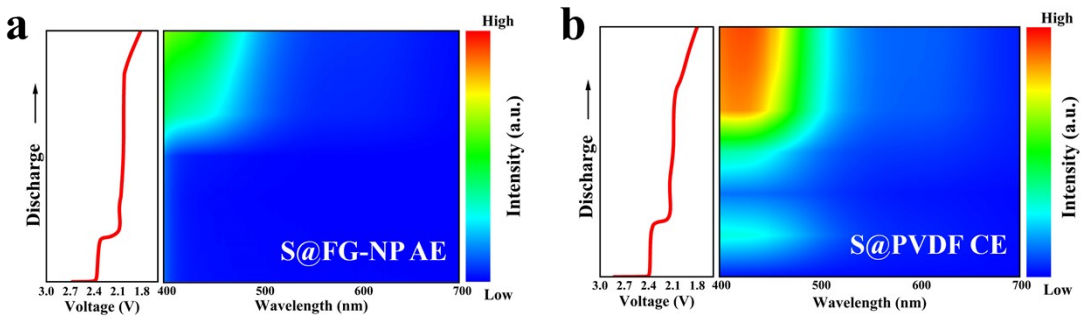

Figure S17 In situ UV-vis spectra during discharging for (a) S@FG-NP AE and (b) S@PVDF CE.

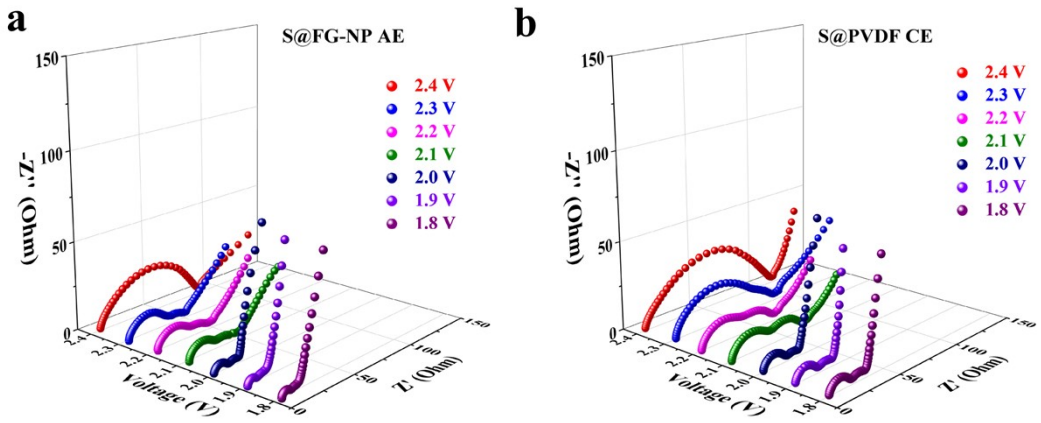

Figure S18 In situ EIS of (a) S@FG-NP AE and (b) S@PVDF CE under different discharging states.

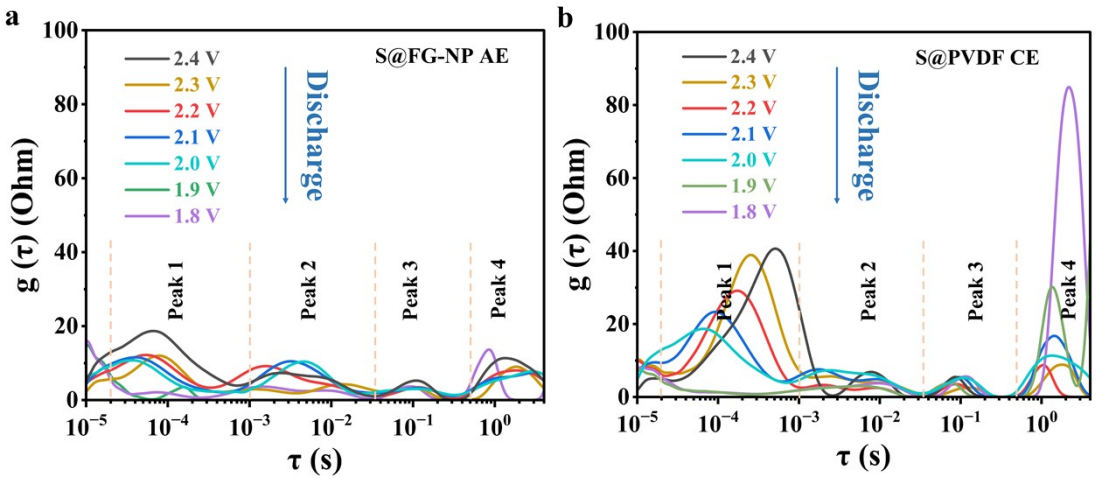

Figure S19 DRT result for (a) S@FG-NP AE and (b) S@PVDF CE from the in-situ EIS.

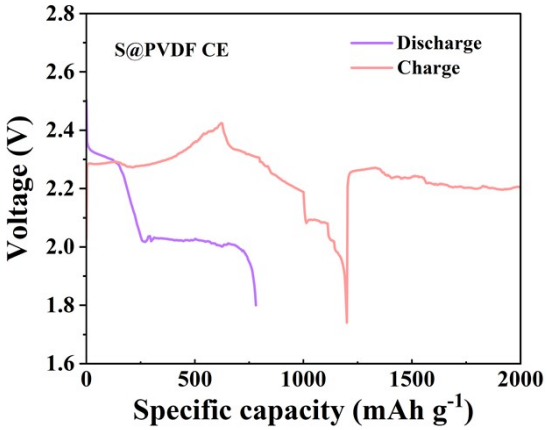

Figure S20 Charge/discharge curves of S@PVDF CE at the 22nd cycle, showing the serious shuttling effect.

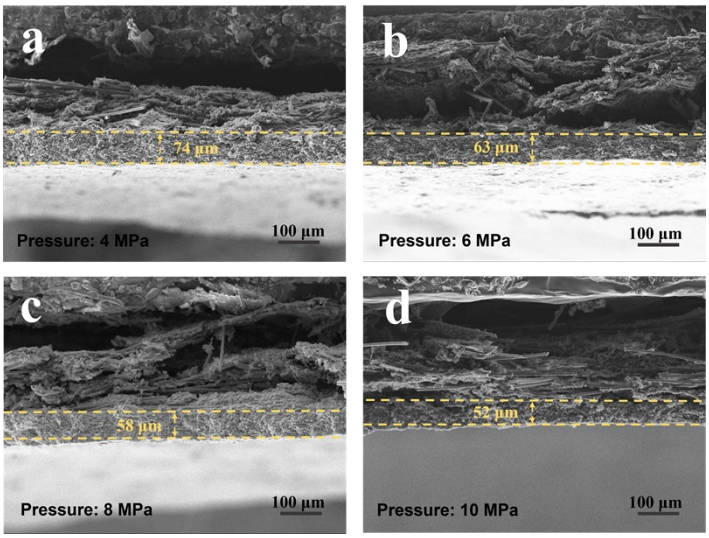

Figure S21 (a-d) Cross-section SEM images of S@FG-NP CE after compaction under different pressures.

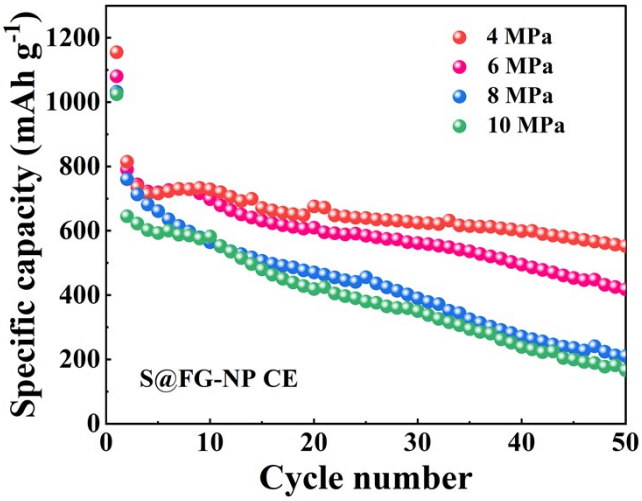

Figure S22 Cycling performance of S@FG-NP CE after compaction under different pressures.

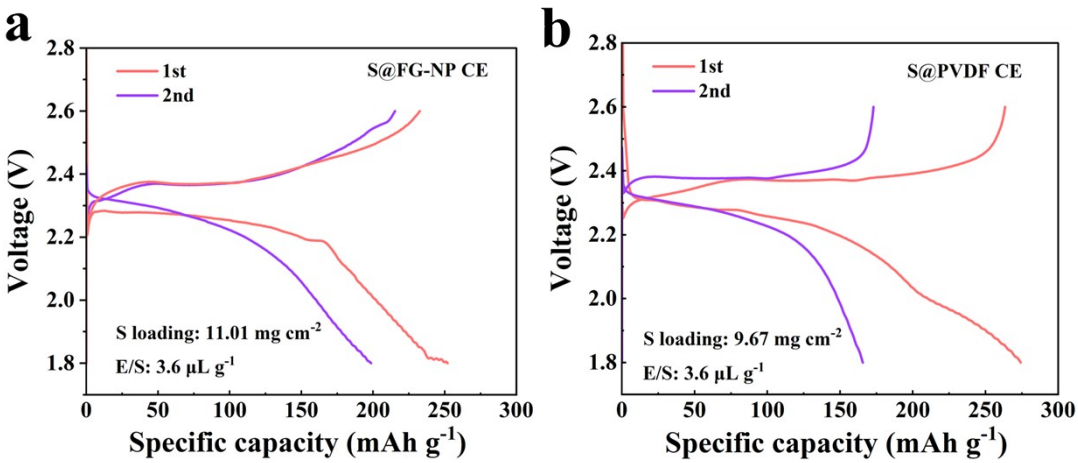

Figure S23 Charge/discharge curves of (a) S@FG-NP CE and (b) S@PVDF CE under lean electrolyte of 3.6 μL mg^{-1}.

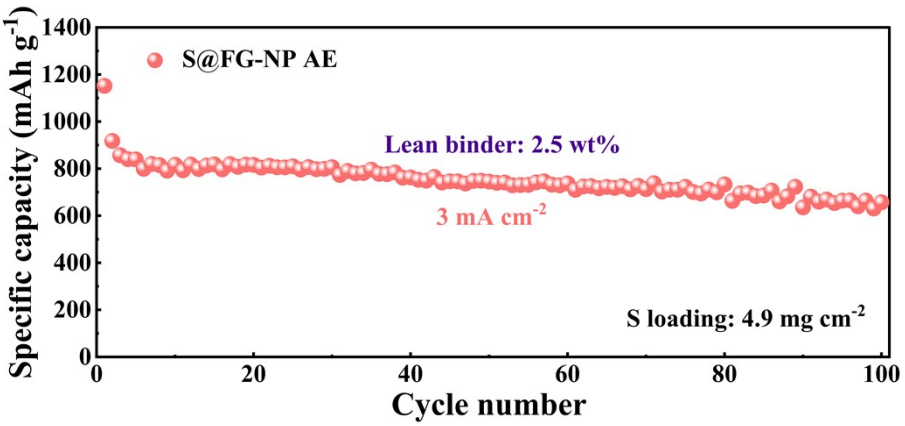

Figure S24 Cycling performance of S@FG-NP AE at a high sulfur loading of 4.9 mg cm^{-2}, employing a lean binder of 2.5 wt% and a high current density of 3 mA cm^{-2}.

Figure S25 Digital photographs of a pouch cell under various bending conditions.

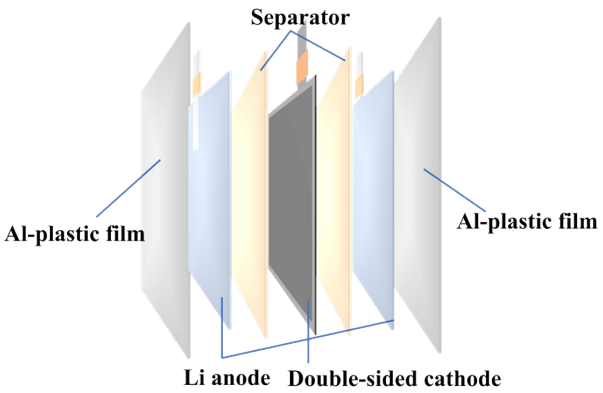

Figure S26 Schematic for the parallel-connection Ah-level Li-S pouch cell.

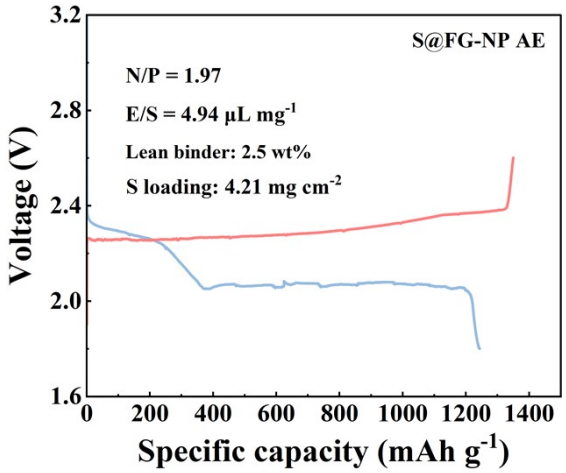

Figure S27 Charge/discharge curves of the Li-S pouch cell with lean binder (2.5 wt%) and low N/P ratio (1.97).

Table S1 Comparison of the rate performance under high sulfur loading with the previously reported works.

Journal	Sulfur loading (mg cm^{-2})	Rate (C)	Areal capacity (mAh cm^{-2})	Specific capacity (mAh g^{-1})	Ref.[a]
Adv. Energy Mater.	4.7	0.1	4.6	978	[67]
ACS Nano	4.0	1	1.7	425	[37]
ACS Nano	4.2	0.2	3.99	950	[66]
Adv. Funct. Mater.	4.2	0.2	4.3	1023	[65]
Adv. Energy Mater.	4	1	2.8	700	[60]
Adv. Sci.	4.5	1	2.007	446	[62]
Nano-Micro Lett.	5.15	1	2.41	468	[63]
Adv. Mater.	4.3	0.5	4.09	951	[59]
Adv. Sci.	4.61	0.2	3.5	759	[35]
ACS Nano	4.2	0.2	3.75	893	[61]
Adv. Funct. Mater.	4.1	0.2	3.34	815	[58]
Nat. Commun.	5	0.5	3.7	736	[56]
	4.6	**0.91**	**3**	**653**	**This work**

[a] References are cited in the main text.

Table S2 Comparison of the sulfur loading and areal capacity under lean electrolyte with the previously reported works.

Binder	Sulfur content (wt%)	Sulfur loading (mg cm^{-2})	E/S (μL mg^{-1})	Areal capacity (mAh cm^{-2})	Ref.[b]
PVBST	56	6.2	7	5.3	[67]
PSPEG	72.96	7.6	4.5	6.47	[34]
LCNF	63.3	13.6	2	12.61	[9]
GB-Y	48	6.56	10	5.23	[54]
FHCP	60	4.72	6	5.25	[18]
PEI-TIC	/	7.1	9	7.2	[52]
P10	49.875	6	4	4.48	[16]
PNAVS	56	11.7	8	12.21	[38]
PVDF/FcBA	48	5	4.3	5	[70]
Mn-COP	49	8.6	7.8	6	[55]
FG-NP	**65**	**10.4**	**3.6**	**9.01**	**This work**

[b] References are cited in the main text.

PVBST: the electrolytephilic soft segments of poly(4-(4-vinylbenzyl)−4H-1,2,4-triazole) (PVBT) and the electrolyte-phobic rigid segments of poly(3-(1-(4-Vinylbenzyl)−1H-imidazol-3-ium-3-yl)-propane-1-sulfonate) (PVBIPS). PSPEG: organo-polysulfide (-S_x-) polymer; LCNF: lignin-containing cellulose nanofibril; GB-Y: gelatin and boric acid-elements (Y); FHCP: toluene diisocynate (TDI), polypropylene glycol-600 (PPG-600), 4,4-dithiodiphenylamine (DTDA), and hexachlorocyclotriphosphazene (HCCP); PNAVS: N-acryloyl glycinamide (NAGA) and 3-(1-vinyl-3-imidazolio) propanesulfonate (VIPS).

Table S3 Performance metrics of the pouch cell with lean binder (2.5 wt%) and low N/P ratio (1.97).

<table>
<tr><th>Size</th><th colspan="2">Double-sided cathode</th><th>Anode</th><th>Separator</th><th>Areal capacity (mAh cm^{-2})</th><th>Gravimetric energy (Wh kg^{-1})</th><th>Volumetric energy (Wh L^{-1})</th></tr>
<tr><td rowspan="4">3×4 cm^2</td><td>Carbon paper (mg)</td><td>S/C/binder (mg)</td><td>Li anode (mg)</td><td>Separator (mg)</td><td rowspan="4">10.5</td><td rowspan="4">791</td><td rowspan="4">618</td></tr>
<tr><td>90.18</td><td>161.84</td><td>64.08</td><td>34.44</td></tr>
<tr><td colspan="4">Pouch cell mass: 350.54 mg</td></tr>
<tr><td colspan="4">Pouch cell thickness: 374 μm</td></tr>
</table>

Gravimetric and volumetric energy densities are systematically calculated by accounting for the mass and volume of the key cell components according to the following formula[1,2]:

$$\text{Gravimetric energy (Wh kg}^{-1}) = \frac{Areal\ capacity\ (mAh\ cm^{-2}) \times\ 2.2V}{Cell\ mass\ (mg\ cm^{-2})} = \frac{10.50\ (mAh\ cm^{-2}) \times\ 2.2V}{29.21\ (mg\ cm^{-2})}$$

$$\text{Volumetric energy (Wh L}^{-1}) = \frac{Areal\ capacity\ (mAh\ cm^{-2}) \times\ 2.2V}{Cell\ thickness\ (\mu m)} = \frac{10.50\ (mAh\ cm^{-2}) \times\ 2.2V}{374\ (\mu m)}$$

Reference:

[1] Z. Chen, T. Chen, J. Wang, P. Li, J. Liu, W. Chen, Z. Yang, Y. Deng, J. Chang, Y. Yang, Adv. Energy Mater. 2024, 34, 2401568.

[2] Z. Chen, M. Lu, Y. Qian, Y. Yang, J. Liu, Z. Lin, D. Yang, J. Lu, X. Qiu, Adv. Energy Mater. 2023, 13, 2300092.